A Compact Airborne G-band (183 GHz) Water Vapor Radiometer and Retrievals of Liquid Cloud Parameters from Coincident Radiometer and Millimeter Wave Radar Measurements

Andrew L. Pazmany[1] and Mengistu Wolde[2]
[1]*ProSensing Inc., Amherst, MA 01002, www.prosensing.com*
T: (413) 549-4402, Email: pazmany@prosensing.com
[2]*Flight Research Laboratory, National Research Council (NRC), Ottawa, Canada*

Introduction

The National Research Council of Canada (NRC), in cooperation with ProSensing Inc., has developed a state-of-the-art dual frequency airborne radar system for atmospheric and flight safety research for its Convair-580 research aircraft. The NRC Airborne W and X-band (NAWX) radar system has polarimetric and Doppler capabilities at both wavelengths and can switch electronically between zenith, nadir and side looking antennas. Using a motorized reflector plate, the zenith W-band antenna is also be able to scan -5° aft to +45° forward in the horizontal and vertical directions, to provide dual-Doppler capability in the side and nadir directions at W-band.

In early 2007 the new NAWX radar system, along with a pod mounted G-band water Vapor Radiometer (GVR) developed by ProSensing Inc. (Pazmany 2007), was installed on the NRC Convair-580 aircraft, as shown in Figure 1, and participated in the Canadian CloudSat and CALIPSO validation flights (C3VP). Liquid cloud data collected with the zenith pointed W-band radar and G-band radiometer, complemented with data from aircraft in situ probes, provided an opportunity to develop and test radar/radiometer algorithms for the estimation of liquid cloud properties. This poster presents a case study of a comparison of W-band and GVR derived cloud properties with that of the measured values from the aircraft cloud physics probes during one of the C3VP flights.

Figure 1. The NRC Convair-580 aircraft with the NAWX radar system and G-band water Vapor Radiometer (GVR).

Approach:

The effective radius, r_{eff} and number concentration, *N* are two important parameters necessary for characterizing liquid cloud properties. For example, these parameters are needed to estimate the energy feedback mechanism between liquid clouds and the boundary layer and the severity of aircraft icing potential in supercooled liquid clouds. *N* and r_{eff} are defined in terms of the cloud drop size distribution, *n(r)* at some height h, according to (Szczodrak *et al*. 2001):

$$N(h)=\int_0^\infty n(r,h)dr, \qquad r_{eff}(h)=\int_0^\infty n(r,h)r^3dr \Big/ \int_0^\infty n(r,h)r^2dr .$$

The zenith pointed GVR measures Liquid Water Path (*lwp*) which is the height integrated Liquid Water Content (*w*), given by

$$w(h)=\frac{4\pi}{3}\int_0^\infty n(r,h)r^3dr \text{ and } lwp=\int_0^\infty w(h)dh.$$

In stratoform clouds, *w* may be estimated from the GVR retrieved *lwp* by flying the aircraft in a porpoise pattern or stepped ascent/descent. The Zenith beam of the W-band radar samples a very similar cloud volume and the measured equivalent radar reflectivity factor, Z_e, for small, Rayleigh cloud droplets can be approximated as the sixth moment of the drop size distribution

$$Z_e(h)=2^6\int_0^\infty n(r,h)r^6dr.$$

From the third and sixth moment of the drop size distribution, a new, *Z*-based estimate of the characteristic cloud drop radius, r_Z may be obtained according to

$$r_Z(h)=\sqrt[3]{\frac{\pi}{48}\frac{Z(h)}{w}}=\sqrt[3]{\int_0^\infty n(r,h)r^6dr \Big/ \int_0^\infty n(r,h)r^3dr}.$$

The difference between r_{eff} and r_Z is primarily a function of the width of the drop size distribution and often can be estimated based on cloud type. Figure 2 illustrates this difference assuming a modified Gamma cloud drop-size distribution for a few cloud types. This figure can be used to estimate r_{eff} from r_Z and then to obtain the effective number density according to:

$$N_{eff}(h)=\frac{3}{4\pi}\frac{w(h)}{r_{eff}^3}.$$

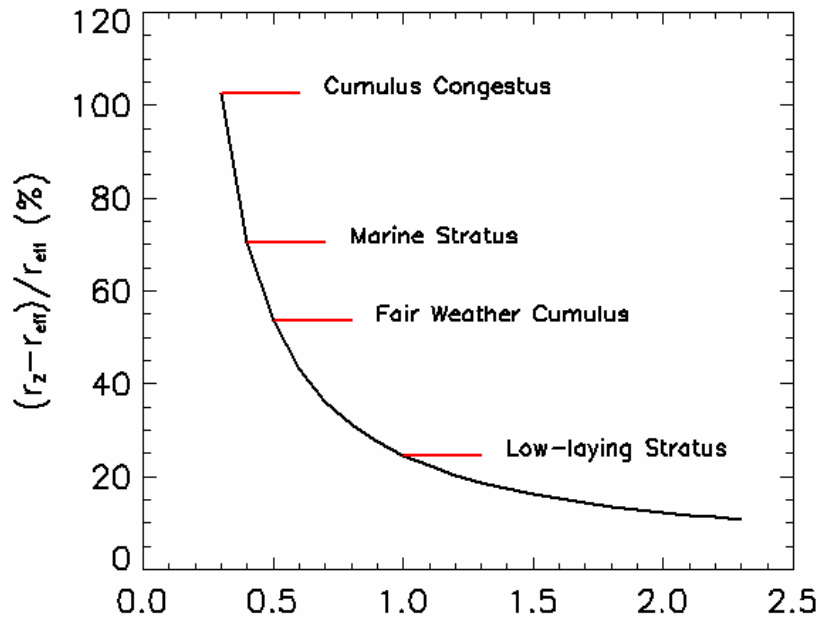

Figure 2. Percent error between effective radius, r_{eff}, and the radar reflectivity based estimate of cloud drop size, r_Z, calculated based on the modified gamma drop-size distribution and cloud parameters tabulated in Ulaby et al.1981 and the marine stratus distribution shape obtained from Vali et al. 1998.

Example Data and Processing:

On January 26, 2007 the NRC Convair 580 sampled a layered cloud system over southeastern Ontario, Canada. The upper cloud layer (>4 km altitude and T < -20°C) was totally glaciated, while the low level layers consisted of regions of glaciated, mixed phase and supercooled liquid clouds. The all-liquid clouds were confined to a shallow (~500 m) inversion layer at the top of the low level cloud deck. The aircraft made repeated porpoise maneuvers in an out of this layer (Fig. 3). Fig 4 shows the GVR and in situ liquid water content (*w*) measurements in the liquid layer. The liquid water content was also estimated from the rate of change in the GVR measured *LWP* as a function of aircraft rate of ascent/descent. Examples of the vertical radar reflectivity cross-section measured by the NAWX W band radar is shown in Fig. 5. Based on the low observed reflectivity and aircraft in situ sensor data, it was assumed that the liquid cloud layer contained small, Rayleigh scattering droplets. From the measured *w* and *Z*, r_Z was estimated, and a 40% difference was applied to obtain r_{eff} by assuming a continental stratus cloud type, with a size distribution width between Cumulus and low lying stratus. Finally the effective number concentration was calculated from *w* and r_{eff}.

The time series plots of LWP and *w* data show consistent measurements. The GVR data show a maximum of up to 0.08 mm at the base of the weak Z cloud layer where *w* is near zero, i.e., the liquid layer is above the aircraft. As the aircraft ascends through the liquid layer, the GVR measured LWP decreases while the in-situ observed *w* data increases. The GVR derived *w* values show a maximum of 0.3 g m^{-3}, which is slightly less than a peak of 0.5 g m^{-3} measured by the in-situ sensor. The GVR derived total particle concentrations (87 and 300 cm^{-3}) also compare well with that measured by the FSSP probe (Fig. 6).

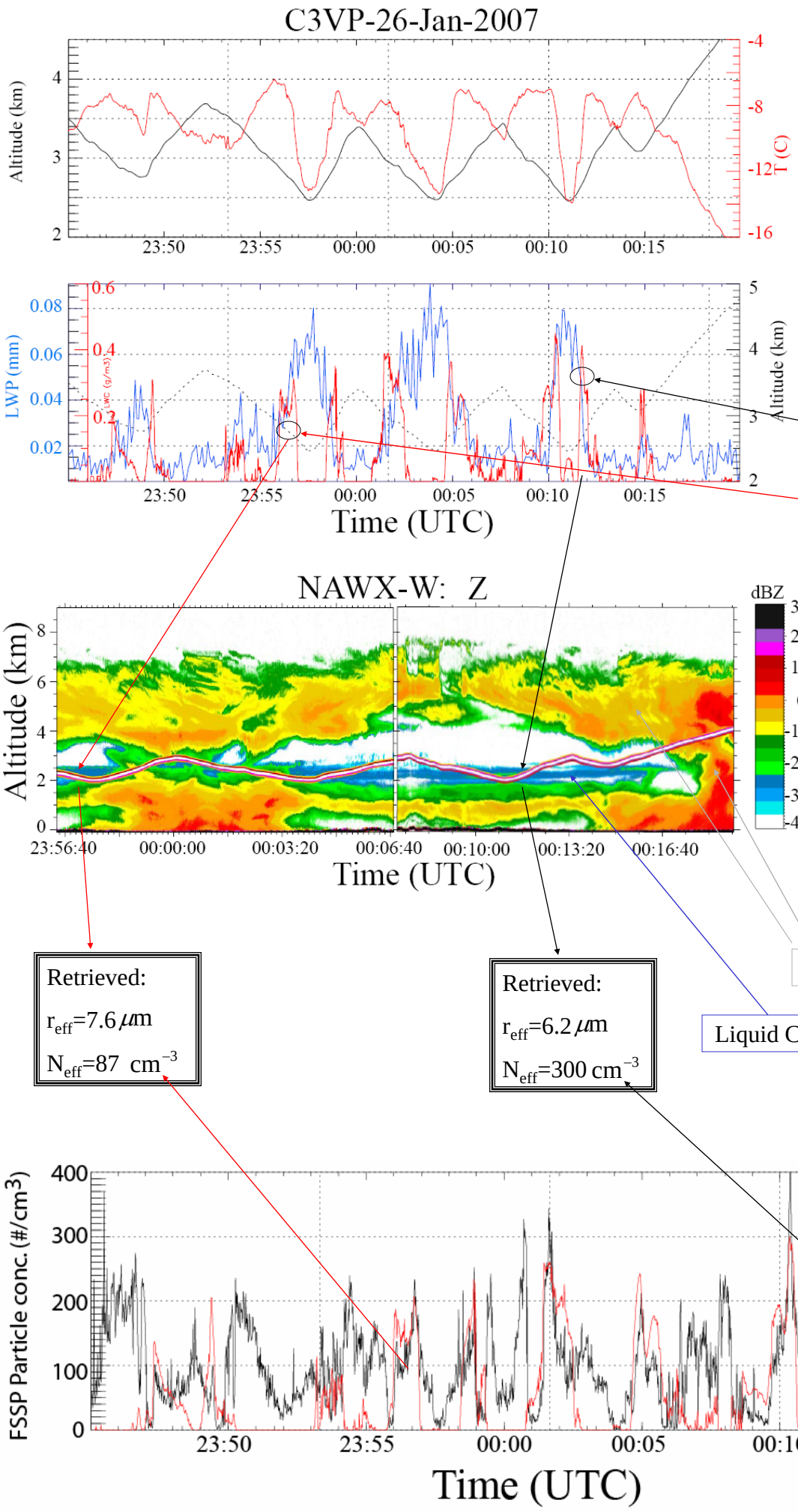

Figure 3. Aircraft altitude (black) and flight level temperature in °C (red) on June 26, 2007.

Figure 4. Aircraft in-situ probe measured liquid water content, *w*, (red) and GVR measured liquid water path (blue). Liquid water content (*w*) was estimated from the GVR LWP data at two data segments as the aircraft changed altitude:

$$w \approx \frac{\Delta LWP}{\Delta h}$$

Figure 5. W-band radar reflectivity image. The nadir and zenith beams were combined to show clouds above and below the aircraft on an absolute altitude above sea level vs. UTC time scale. The aircraft flight path is indicated with a double red line in the image.

Figure 6. Time series of particle concentrations measured by an FSSP and liquid water content measured by a king probe.

References:

Pazmany, A. L., "A compact 183-GHz radiometer for water vapor and liquid water sensing" *IEEE Trans. Geosci.. Remote Sens.* Vol. 45, No. 7, pp. 2202-2206, July 2007.

Szczodrak, M., P. H. Austin, P. B. Krummel, "Variability of optical depth and effective radius in marine stratocumulus clouds" J. Atmos. Sci., Vol 58, pp. 2912-2926, 2001.

Ulaby, F. T., R. K. More and A. K. Fung, "Microwave Remote Sensing", Vol. 1, *Addision-Wesley Publishing Co.*, 1981.

Vali, G., R. D. Kelly, J. French, S. Haimov, D. Leon, R. E. McIntosh and A. L. Pazmany, "Finescale structure and microphysics of coastal stratus", Vol. 55, No. 24, pp. 3540-3564, Dec. 1998.